REPORT DOCUMENTATION PAGE

Form Approved OMB NO. 0704-0188

1. REPORT DATE (DD-MM-YYYY)	2. REPORT TYPE	3. DATES COVERED (From - To)
02-04-2011	Final Report	1-Sep-2007 - 31-Dec-2010

4. TITLE AND SUBTITLE

Towards High-Efficiency Mid-Infrared Diode Lasers Operating From 3-5 Microns

5a. CONTRACT NUMBER
W911NF-07-1-0528

5b. GRANT NUMBER

5c. PROGRAM ELEMENT NUMBER
611102

6. AUTHORS
Seth R. Bank

5d. PROJECT NUMBER

5e. TASK NUMBER

5f. WORK UNIT NUMBER

7. PERFORMING ORGANIZATION NAMES AND ADDRESSES
University of Texas at Austin
The University of Texas at Austin
101 East 27th Street
Austin, TX 78712 -1500

8. PERFORMING ORGANIZATION REPORT NUMBER

9. SPONSORING/MONITORING AGENCY NAME(S) AND ADDRESS(ES)
U.S. Army Research Office
P.O. Box 12211
Research Triangle Park, NC 27709-2211

10. SPONSOR/MONITOR'S ACRONYM(S)
ARO

11. SPONSOR/MONITOR'S REPORT NUMBER(S)
53255-EL.1

12. DISTRIBUTION AVAILIBILITY STATEMENT
Approved for Public Release; Distribution Unlimited

13. SUPPLEMENTARY NOTES
The views, opinions and/or findings contained in this report are those of the author(s) and should not contrued as an official Department of the Army position, policy or decision, unless so designated by other documentation.

14. ABSTRACT
We have actively pursued GaSb-based dilute-nitride diode lasers to cover the 3-5 micron regime. We significantly advanced the growth understanding of GaSb-based dilute-nitride lasers, culminating in the first observation of room-temperature photoluminescence from a GaSb-based dilute-nitride quantum well. While the growth of these metastable alloys is challenging, we have identified a critical new issue governing the ultimate performance of these devices: free-carrier absorption. Moreover, researchers already face this issue at shorter wavelengths (~ 3

15. SUBJECT TERMS
Molecular Beam Epitaxy, Dilute-Nitride Semiconductors, Mid Infrared Lasers

16. SECURITY CLASSIFICATION OF:			17. LIMITATION OF ABSTRACT	15. NUMBER OF PAGES	19a. NAME OF RESPONSIBLE PERSON
a. REPORT	b. ABSTRACT	c. THIS PAGE			Seth Bank
UU	UU	UU	UU		19b. TELEPHONE NUMBER 512-471-9669

Report Title

Towards High-Efficiency Mid-Infrared Diode Lasers Operating From 3-5 Microns

ABSTRACT

We have actively pursued GaSb-based dilute-nitride diode lasers to cover the 3-5 micron regime. We significantly advanced the growth understanding of GaSb-based dilute-nitride lasers, culminating in the first observation of room-temperature photoluminescence from a GaSb-based dilute-nitride quantum well. While the growth of these metastable alloys is challenging, we have identified a critical new issue governing the ultimate performance of these devices: free-carrier absorption. Moreover, researchers already face this issue at shorter wavelengths (~ 3 microns). We have invented a novel method for mitigating these losses, specifically GaSb/ErSb/GaSb tunnel junctions, which we have developed through an Add-On Award. We have also developed a prototype GaInAsSb/AlGaAsSb laser structure to serve as a testbed for examining dilute-nitride active regions, as well as the novel tunnel junction device structure.

List of papers submitted or published that acknowledge ARO support during this reporting period. List the papers, including journal references, in the following categories:

(a) Papers published in peer-reviewed journals (N/A for none)

A.M. Crook, H.P. Nair, S.R. Bank, "Surface segregation effects of erbium in GaAs growth and their implications for optical devices containing ErAs nanostructures," Appl. Phys. Lett., vol. 98, pp. 121108-1-3, March 2011.

A.M. Crook, H.P. Nair, S.R. Bank, "Investigating the Optical Quality of ErAs Nanoparticle-Enhanced Tunnel Junctions," Phys. Status Solidi C, DOI 10.1002/pssc.200983914, June 2010.

H.P. Nair, A.M. Crook, S.R. Bank, "Low-Resistance GaAs-Based Tunnel Junctions Enhanced with Semimetallic Nanoparticles," Appl. Phys. Lett., vol. 96, pp. 222104-1-3, May 2010.

Number of Papers published in peer-reviewed journals: 3.00

(b) Papers published in non-peer-reviewed journals or in conference proceedings (N/A for none)

Number of Papers published in non peer-reviewed journals: 0.00

(c) Presentations

A.M. Crook, H.P. Nair, D.A. Ferrer, S.R. Bank, “Growth of Epitaxially-Embedded ErAs Films in GaAs,” To be presented at the 53rd Electronic Materials Conf. (EMC), June 2011, Santa Barbara, CA.

R. Salas, E.M. Krivoy, A.M. Crook, H.P. Nair, S.R. Bank, “Improved conductivity of GaAs-based tunnel junctions containing ErAs nanostructures via compositional grading,” To be presented at the 53rd Electronic Materials Conf. (EMC), June 2011, Santa Barbara, CA.

H.P. Nair, A.M. Crook, S.R. Bank, “An Epitaxial Metal/Semiconductor System for Active Plasmonic Devices,” To be presented at the 2011 Conf. on Lasers and Electro Optics (CLEO), May 2011, Baltimore, MD.

A.M. Crook, H.P. Nair, S.R. Bank, “Nanoparticle-Enhanced Tunnel Junctions for Reduced Free-Carrier Absorption in Mid-IR Lasers,” To be presented at the 2011 Conf. on Lasers and Electro Optics (CLEO), May 2011, Baltimore, MD.

K.W. Park, H.P. Nair, A.M. Crook, V.D. Dasika S.R. Bank, E.T. Yu, “Scanning Probe Microscopy Studies of GaAs pn Junctions with Embedded ErAs Nanoparticles,” 38th Conference on the Physics and Chemistry of Surfaces and Interfaces (PCSI), Jan. 2011, San Diego, CA.

A. M. Crook, H. P. Nair, K. W. Park, E. T. Yu, S.R. Bank, “Investigating the MBE Overgrowth of Semimetallic Nanoparticles for Nanophotonics,” 2010 North American Molecular Beam Epitaxy Conf. (NAMBE), Sept. 2010, Breckenridge, CO.

H. P. Nair, A. M. Crook, K. W. Park, D. A. Ferrer, S. K. Banerjee, E. T. Yu, S.R. Bank, “Investigation of MBE-grown ErAs nanoparticle morphology for high- performance optical and electronic devices,” 2010 North American Molecular Beam Epitaxy Conf. (NAMBE), Sept. 2010, Breckenridge, CO.

A.M. Crook, H.P. Nair, K.W. Park, E.T. Yu, S.R. Bank, “Overgrowth Investigation of Epitaxial Semimetallic Nanoparticles for Photonic Devices,” 52nd Electronic Materials Conf. (EMC), June 2010, South Bend, IN.

K.W. Park, A.M. Crook, H.P. Nair, S.R. Bank, E.T. Yu, “Scanned Probe Characterization of Self-Assembled ErAs/GaAs Semimetal/Semiconductor Nanostructures Grown by Molecular Beam Epitaxy,” 52nd Electronic Materials Conf. (EMC), June 2010, South Bend, IN.

(Invited) S.R. Bank, A.M. Crook, H.P. Nair, “Nanoparticle-enhanced tunnel junctions for high-efficiency solar cells and mid-infrared lasers,” 216th Electrochemical Society Conference, Oct. 2009, Vienna, Austria.

A.M. Crook, H.P. Nair, S.R. Bank, “High-Performance Metal Nanoparticle-Enhanced Tunnel Junctions for Photonic Devices,” International Symposium on Compound Semiconductors (ISCS), Sept. 2009, Santa Barbara, CA.

A.M. Crook, H.P. Nair, K. Vijayraghavan, M.A. Wistey, J.D. Zimmerman, J.M.O. Zide, A.C. Gossard, S.R. Bank, “Annealing Stability of Nanoparticle-Enhanced Tunnel Junctions for High-Efficiency Solar Cells and Mid-Infrared Lasers,” 51st Electronic Materials Conf. (EMC), June 2009, University Park, PA.

(Invited) S.R. Bank, “Enhancing Diode Lasers with Metallic Nanoparticles,” IEEE Photonics Semiconductor Laser Workshop, June 2009, Baltimore, MD.

H.P. Nair, A.M. Crook, J. M. O. Zide, M.P. Hanson, A.C. Gossard, S.R. Bank, “Nanoparticle-enhanced tunnel junctions for high efficiency mid-infrared lasers,” 50th Electronic Materials Conf. (EMC), June 2008, Santa Barbara, CA.

Number of Presentations: 14.00

Non Peer-Reviewed Conference Proceeding publications (other than abstracts):

Number of Non Peer-Reviewed Conference Proceeding publications (other than abstracts): 0

Peer-Reviewed Conference Proceeding publications (other than abstracts):

Number of Peer-Reviewed Conference Proceeding publications (other than abstracts): 0

(d) Manuscripts

K.W. Park, A.M. Crook, H.P. Nair, S.R. Bank, E.T. Yu, "Scanned Probe Characterization of Self-Assembled ErAs/GaAs Semimetal/Semiconductor Nanostructures Grown by Molecular Beam Epitaxy," Submitted to Appl. Phys. Lett., 2011.

Number of Manuscripts: 1.00

Patents Submitted

Patents Awarded

Awards

Kavli Fellow (2010)
ONR Young Investigator Program (YIP) (2010)
NSF Faculty Early Career Development (CAREER) Program (2010)
AFOSR Young Investigator Program (YIP) (2009)
Presidential Early Career Award for Scientists and Engineers (PECASE) (2009)
Young Scientist Award from the International Conf. on Compound Semiconductors (ISCS) (2009)
Young Investigator Award from North American Conf. on Molecular Beam Epitaxy (NAMBE) (2008)
DARPA Young Faculty Award (YFA) (2008)

Graduate Students

NAME	PERCENT_SUPPORTED
Hari Nair	1.00
Adam Crook	0.17
FTE Equivalent:	**1.17**
Total Number:	**2**

Names of Post Doctorates

NAME	PERCENT_SUPPORTED
FTE Equivalent:	
Total Number:	

Names of Faculty Supported

NAME	PERCENT_SUPPORTED	National Academy Member
Seth Bank	0.00	No
FTE Equivalent:	**0.00**	
Total Number:	**1**	

Names of Under Graduate students supported

NAME	PERCENT_SUPPORTED
FTE Equivalent:	
Total Number:	

Student Metrics

This section only applies to graduating undergraduates supported by this agreement in this reporting period

The number of undergraduates funded by this agreement who graduated during this period:	0.00
The number of undergraduates funded by this agreement who graduated during this period with a degree in science, mathematics, engineering, or technology fields:.....	0.00
The number of undergraduates funded by your agreement who graduated during this period and will continue to pursue a graduate or Ph.D. degree in science, mathematics, engineering, or technology fields:.....	0.00
Number of graduating undergraduates who achieved a 3.5 GPA to 4.0 (4.0 max scale):	0.00
Number of graduating undergraduates funded by a DoD funded Center of Excellence grant for Education, Research and Engineering:	0.00
The number of undergraduates funded by your agreement who graduated during this period and intend to work for the Department of Defense	0.00
The number of undergraduates funded by your agreement who graduated during this period and will receive scholarships or fellowships for further studies in science, mathematics, engineering or technology fields:	0.00

Names of Personnel receiving masters degrees

NAME
Hari Hair
Adam Crook
Total Number: 2

Names of personnel receiving PHDs

NAME
Total Number:

Names of other research staff

NAME	PERCENT_SUPPORTED
FTE Equivalent:	
Total Number:	

Sub Contractors (DD882)

Inventions (DD882)

Scientific Progress

See Attachment

Technology Transfer

1. Abstract

In light of the theoretical and experimental advances developed throughout the program, we have focused our efforts along three main experimental vectors: (1) developing high-quality GaSb-based dilute-nitride active regions, (2) demonstrating the first ErSb nanoparticle-enhanced tunnel junctions for low-loss laser structures, and (3) developing a nitrogen-free AlGaAsSb/InGaAsSb laser structure that is compatible with incorporating dilute-nitride active regions (i.e. grown at low temperatures) and ErSb nanoparticle-enhanced tunnel junctions. We review the progress in all three areas, which indicate that high-performance mid-IR dilute-nitride lasers are now achievable.

We have, for the first time, achieved a generalized understanding of dilute-nitride growth, which is necessary because of the differences between GaSb-based dilute-nitrides and the conventional GaAs-based dilute-nitrides. These insights, developed in the course of this program, enabled the first demonstration of room temperature photoluminescence of GaSb-based dilute-nitrides (previous reports have only been at low temperatures).

We have also demonstrated the first ErSb nanoparticle-enhanced tunnel junctions on GaSb and have found that – even with very low p-doping – the tunnel junctions have sufficient conductivity for laser applications. This is a very exciting development as we now have a path to greatly reduce the internal loss of GaSb-based diode lasers, without compromising the electrical characteristics (i.e. electrical resistance).

We have developed and grown an AlGaAsSb/InGaAsSb laser structure, targeting λ~2.8 μm, to use as a testbed for the dilute-nitride active regions and the tunnel junctions.

2. Growth of High-Quality Dilute-Nitride Materials

Achieving high optical quality is essential for incorporating dilute-nitride active regions into mid-IR lasers. We have previously achieved high structural quality GaNSb, containing up to 1.8% nitrogen (**Fig. 1**). We have identified the major causes of optical quality degradation in dilute-nitride antimonides and have addressed many of them in this program. In particular, we believe that we have definitively identified the ideal growth regime for GaSb-based dilute-nitride active regions, for the first time. The growth window differs significantly from that of the GaAs-based dilute-nitrides, which has necessitated that we fundamentally re-engineer our approach to growing dilute-nitrides – the result is the first generalized understanding of the growth space of this important class of materials.

First, there is the issue of optimal plasma operating parameters, which involves optimizing three main variables, namely, plasma power, flow-rate, and deflector plate voltage. These three parameters need to be optimized simultaneously, as changing any one affects the other two. There are several reports of optimal plasma conditions (power/flow combinations) in the literature, and we have been operating our plasma cell under these conditions. These conditions minimize the energy of ions and neutral species that are emitted from the plasma cell. After choosing a power/flow combo that generates the least energetic ions and neutral species, we prevent the ions from reaching the substrate by using dc-biased deflector plates. The voltage applied to the deflector plates was optimized using photoluminescence (PL) structures of GaNAs QWs, embedded in GaAs.

The second major – and more formidable – cause for degradation in the optical quality of dilute-nitride antimonides is the fraction of nitrogen that incorporates as interstitials. Consistent with literature, and confirmed by our high-resolution X-ray diffraction (HR-XRD) and secondary ion mass spectrometry (SIMS) studies, we have determined that a major fraction of the non-substitutional nitrogen incorporates as Sb-N split interstitials, if the growth conditions are non-optimal. The Sb-N interstitial dilates while substitutional N shrinks the lattice. Hence, the formation of Sb-N nitrogen is energetically favorable at the growth front to minimize strain. Therefore, using HR-XRD alone to determine the total N incorporation provides misleading results. We believe that N initially incorporates

substitutionally but then tends to surface segregate and form Sb-N interstitials, if sufficient energy is available. The formation of Sb-N interstitial in dilute-nitride-antimonides is substantially stronger issue than the formation of As-N interstitials in the case of dilute-nitride-arsenides, due to the greater Sb-N bond strength and proportional strain reduction (greater electronegativity mismatch between Sb and N). This can be observed indirectly because the GaAs surface can be driven nitrogen-rich and phase segregates at high growth temperatures, while the GaSb surface does not become nitrogen-rich, indicating that the surface segregating nitrogen atoms incorporate into the lattice in some other form (Sb-N split interstitials). We also believe the large fraction of Sb-N split interstitials is responsible for the p-type doping of GaNSb with large nitrogen concentrations, as seen in literature.

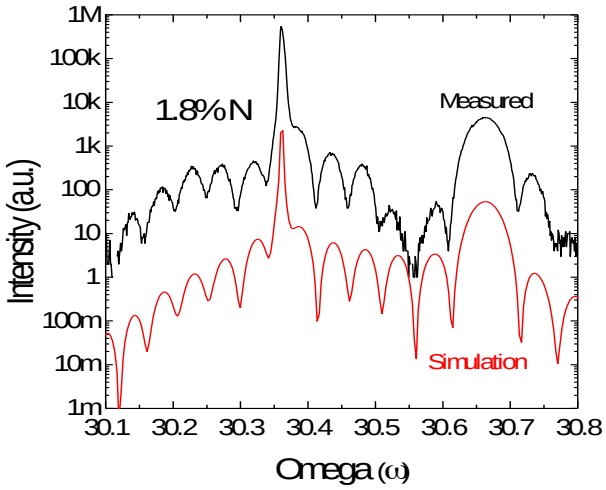

Figure 1. HR-XRD around the (004) reflection (black curve) and simulation (red curve) for a 100 nm thick GaNSb layer.

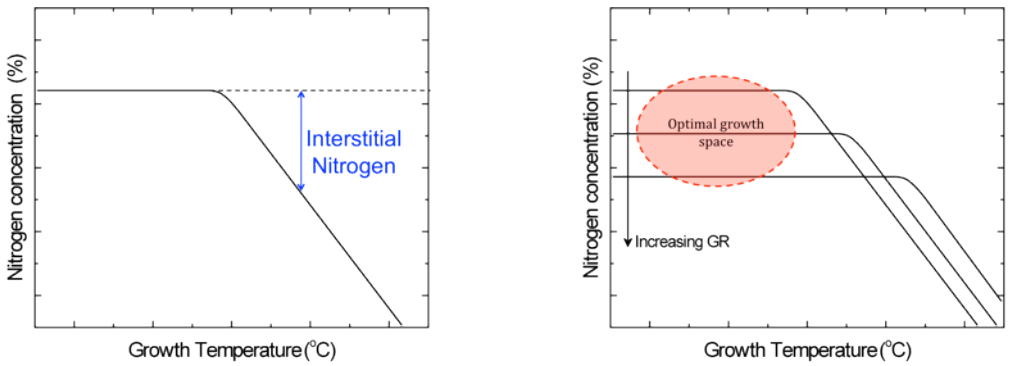

Figure 2. (a) Sketch of substitutional nitrogen incorporation, with growth temperature. Higher growth rates and lower growth temperatures kinetically limit undesirable interstitial nitrogen incorporation. (b) Generalized picture of nitrogen incorporation, illustrating the dependence on growth rate (GR). The ideal growth window is highlighted in red.

Our generalized view of the growth parameter space of dilute-nitrides is summarized in **Figs. 2a** and **b**, where the growth must be sufficiently kinetically limited that the nitrogen incorporation (determined with HR-XRD) is independent of growth temperature – in other words, nitrogen incorporates entirely substitutionally. At elevated temperatures, the apparent nitrogen incorporation

increases because of split interstitial formation, degrading optical quality (blue arrow in **Fig. 2a**). It is clear from the experimental data in **Fig. 3a** and **3b** that both lowering the growth temperature and increasing the growth rate kinetically limit this surface segregation process, decreasing the fraction of Sb-N interstitials. From this, we have concluded that the optimal growth space that minimizes Sb-N interstitials is when the percentage of nitrogen incorporation measured using XRD becomes temperature independent, as seen under certain growth conditions in **Figs. 3a** and **3b**. Reducing the nitrogen flux (**Fig. 3b**, blue curve) enabled us to reach the growth regime where the nitrogen incorporation becomes completely independent of growth temperature. Further studies involving SIMS and Nuclear Reaction Analysis Rutherford Backscattering Spectrometry (NRA-RBS) are underway to confirm that this growth regime indeed minimizes the fraction of non-substitutional nitrogen.

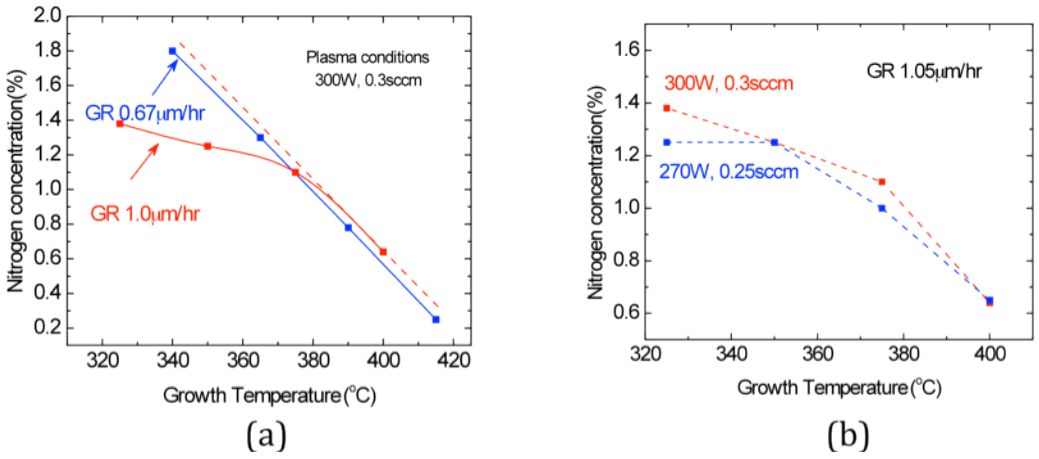

Figure 3. (a) Nitrogen incorporation trend with growth temperature, measured using HR-XRD, for different growth rates. Higher growth rates and lower growth temperatures kinetically limit interstitial nitrogen incorporation. (b) Nitrogen incorporation with growth temperature, measured using HR-XRD, for different plasma conditions. Lower nitrogen flux leads to more complete substitutional incorporation of nitrogen, for a given growth temperature and growth rate.

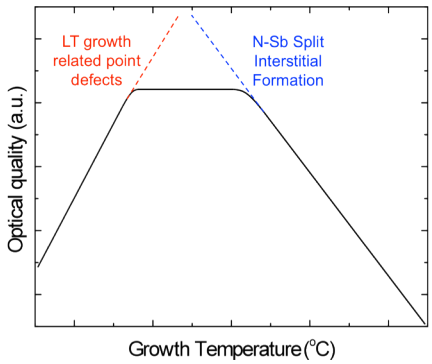

Figure 4. Complete picture of the optical quality of dilute-nitrides, versus growth temperature (shown for a given growth rate and optimized plasma conditions). The growth temperature is limited on the low end by point defect formation and on the high end by split interstitial formation.

We have identified the growth space that minimizes the fraction of interstitial nitrogen species, enabling the first high optical quality dilute-nitride antimonides. In the future, we must optimize the growth window further because, as sketched in **Fig. 4**, growth at too low temperatures results in point defect formation that also degrades the optical quality. However, after identifying the general growth

window for dilute-nitride-antimonides, we proceeded to develop active regions grown under these optimal conditions. Unfortunately the optical quality remained poor yielding no room temperate PL, consistent with other literature reports, despite mitigating Sb-N split interstitial formation. For nitrogen atoms to surface segregate, they require some source of energy to overcome the potential barrier for segregation. Reducing the substrate temperature eliminated this source of energy for the surface segregating nitrogen atoms.

Since optical quality did not improve, we examined whether there were some other impurities originating from our nitrogen plasma source, which could be degrading the optical quality. To this end, we carefully baked and leak-checked the nitrogen gas delivery manifold samples and then grew a structure where the plasma source was running but the nitrogen shutter was kept closed to see if there were significant quantities of background impurities, using the sample structure shown in **Fig. 5a**. As seen in **Fig. 5b**, the degradation in optical quality was small and could not explain the dramatic degradation in optical quality when the nitrogen shutter was left open for growing a dilute-nitride layer.

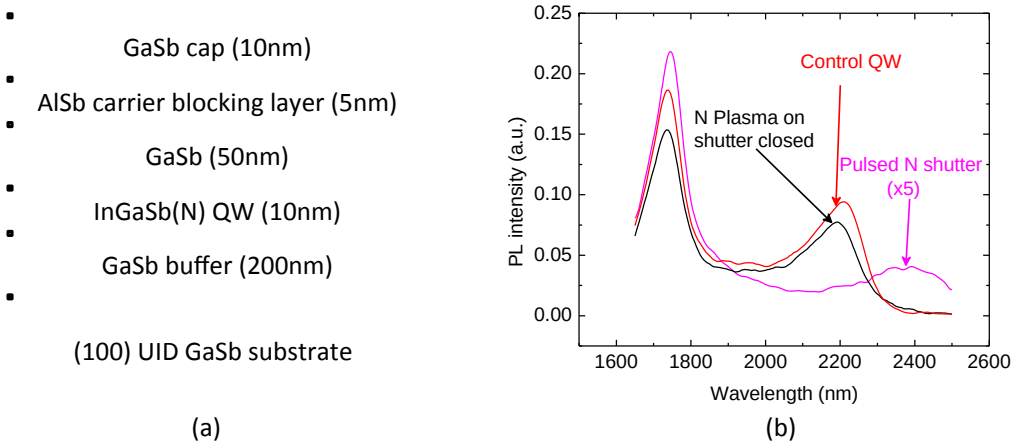

Figure 5. (a) Layer structure for optical quality studies. (b) PL spectra including the first room-temperature PL emission from a dilute-nitride-antimonide active region on GaSb, using the nitrogen pulsing technique.

Our subsequent hypothesis was that there must be some other source of energy helping the surface segregation of nitrogen atoms. The nitrogen plasma source generates highly energetic species during operation. The ions can be filtered out electrostatically using deflection plates; however, the energetic neutrals can impinge on the substrate and provide energy for the surface segregation of nitrogen atoms. To investigate this, we developed a novel technique for incorporating nitrogen, while minimizing the amount of energetic species impinging on the substrate. Our technique involves opening the nitrogen shutter for very short durations so that the nitrogen atoms already on the substrate surface do not get bombarded by the energetic neutrals from the plasma source. This resulted in the first room-temperature PL (**Fig. 5b**) from an InGaSb(N) QW, grown on GaSb. This is an incredibly exciting result that indicates that dilute-nitride-antimonide materials are excellent candidates for extending the emission wavelength of mid-IR diode lasers. Work is currently underway to couple these new growth techniques with the high-performance, 2.8 μm, InGaAsSb/InAlAsSb active region that we have developed, to extend the emission wavelength >3 μm.

Samples were grown on a Varian Gen II MBE system equipped with an SVTA rf plasma cell as a source of active nitrogen. The plasma conditions were monitored using optical intensity measurements and the plasma power was controlled to keep optical intensity constant. Indium, gallium and aluminum were evaporated from conventional solid sources and antimony was supplied from a valved cracker where the cracker temperature was kept high enough to ensure the formation of monomeric antimony.

The antimony to V/III beam-equivalent pressure ratio was 2.3x. The nitrogen plasma source was run at an rf power level of 195 W and 0.18 sccm nitrogen flow rate. The QWs were grown at a substrate temperature of 310˚C, which we found to maximize the incorporation of substitutional nitrogen (i.e. minimizing the formation of N-Sb split interstitials). For the dilute nitride samples the plasma was ignited during the growth of the GaSb buffer so that the plasma had enough time to stabilize. During the growth of the InGaSb QW we used a pulsed nitrogen technique to incorporate active nitrogen into the QW. This involves opening the nitrogen shutter for only 1 monolayer in the middle of the InGaSb QW. Upon opening the shutter a certain dose of active nitrogen impinges on the substrate surface, but upon closing the shutter we eliminate energetic species from the plasma cell reaching the substrate. These energetic nitrogen species could potentially promote the surface segregation of the nitrogen atoms already on the surface, promoting the formation of Sb-N split interstitials and degrading the optical quality. During this investigation, we have developed a unified model for the origin of degradation in optical quality in all dilute-nitrides (nitride-antimonides and nitride-arsenides) through nitrogen surface segregation and subsequent formation of split interstitials.

Room temperature PL was used to characterize these samples. A diode-pumped solid-state (DPSS) laser operating at 532 nm was used as a pump source. The pump laser was modulated using a chopper wheel and the PL signal was collected, collimated and sent through a spectrometer fitted with an InSb detector operating at 77K. The voltage signal from the InSb detector was connected to a lock-in amplifier to perform phase sensitive detection. We believe that by further exploring this growth parameter space, high-quality dilute-nitride active regions operating in the mid-IR region can be realized.

3. Nanoparticle-Enhanced Tunnel Junctions

Numerous challenges conspire to make extension of the lasing wavelength of type-I diode lasers difficult [2]. Dilute-nitride active regions can address many of these issues (Auger recombination, carrier leakage, etc.); however, a complimentary approach, at the device structure level, is required to mitigate the increase in optical absorption, with wavelength, by free holes. This is particularly important at longer wavelengths as the Auger recombination rate scales as the cube of the threshold carrier concentration, while the radiative emission scales with only the square of carrier concentration. Therefore, a small reduction in threshold carrier concentration, due to optical absorption, can greatly degrade the overall performance of long-wavelength lasers – far more than from simple external efficiency considerations.

Figure 6 (a-d) summarizes our general approach (described in detail in last year's report), to reduce the number of holes in the laser structure, reducing the internal loss in proportion. Beginning with the standard p-cladding layer employed in Ref. [1] (**Fig. 6a**), we systematically reduce the number of holes and absorption loss by (**Fig. 6b**) replacing the p-cladding with an n-cladding and a tunnel junction, (**Fig. 6c**) enhancing the tunnel junction with ErSb metal nanoparticles, and (**Fig. 6d**) straining the thin p-layer. **Figure 6e** summarizes the potential >4x reduction in absorption loss, with what have turned out to be conservatively low p-doping densities.

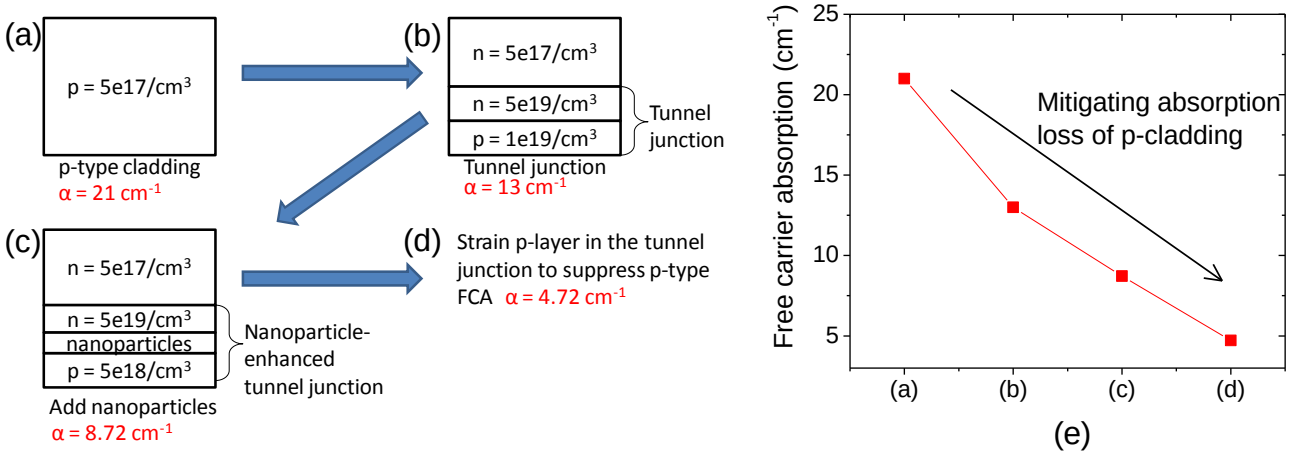

Figure 6. Mitigating absorption losses in the p-type cladding of GaSb-based GaIn(N)AsSb/AlGaAsSb lasers. (a) Conventional approach of a p-doped top cladding [1]. (b) Replacing the p-cladding with an n-cladding and a p^+/n^+ tunnel junction reduces the loss significantly while maintaining virtually identical electrical characteristics. (c) Addition of ErSb nanoparticles at the tunnel junction interface enhances tunneling ~10^5x, allowing the p-doping to be reduced substantially. (d) Straining the (thin) p^+ layer in the tunnel junction alters the energy band structure, reducing the p-type free carrier absorption loss. (e) Summary of (a)–(d) showing the path to high-efficiency mid-IR laser diodes.

As shown in **Fig. 7**, we have demonstrated the first ErSb nanoparticle-enhanced tunnel junctions in GaSb. These tunnel junctions are sufficient to reduce the optical loss associated with the p-type cladding by >10 cm^{-1} (>60% of internal loss) without compromising the electrical conductivity (1 kA/cm^2 at ~0.25 V bias), even for a more conservative p-doping of $1x10^{18}$ cm^{-3} (5x lower than in the calculations shown in **Fig. 6**). **Figure 7** plots the tunnel junction current-density versus voltage for ErSb nanoparticle-enhanced GaSb-based tunnel junctions, for various p-type doping concentrations. Additionally, the ErSb nanoparticle morphology has not been optimized for minimal p-type doping, so further reduction in the required doping level may be realized by utilizing larger nanoparticles.

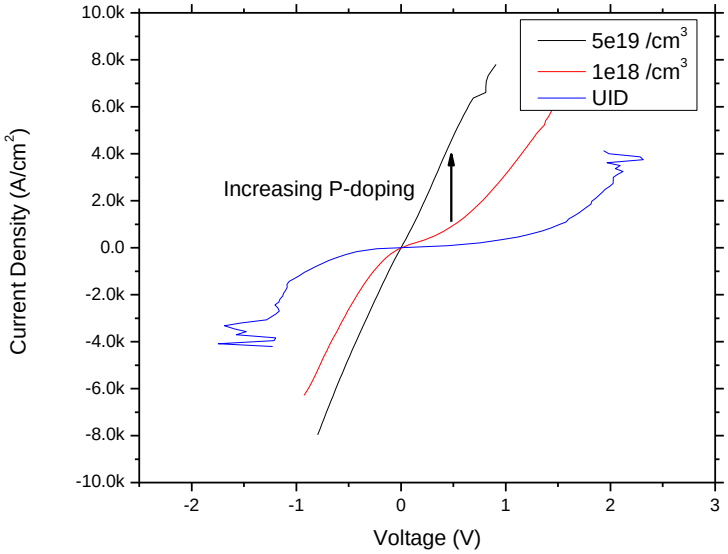

Figure 7. Tunnel junction current density, versus voltage for varying doping concentrations in GaSb tunnel junctions, enhanced with ErSb nanoparticles. Note that only a modest p-doping of $1x10^{18}$ cm^{-3} (red curve) is required for low-resistance tunnel junctions.

4. Development of an AlGaAsSb/InGaAsSb Laser Prototype

In order to demonstrate the material advantages of dilute-nitride active regions and ErSb nanoparticle-enhanced tunnel junction claddings, we must begin with a high-quality GaSb-based laser to function as a testbed. High-performance AlGaAsSb/GaInAsSb lasers have been demonstrated in the 2-3 μm range and we have developed and grown laser structures that are expected to yield competitive device performance, while still being compatible with dilute-nitride and ErSb growth [2].

Because MBE growth is generally performed in the group-V stabilized growth regime (where group-III elements have unity sticking coefficients), it is relatively straight forward to control the group-III alloy compositions. Unfortunately, this is not the case for controlling group-V alloy compositions, such as AlGaAsSb and InGaAsSb. Several methods have been reported as possible ways for controlling the alloy composition but an exhaustive study with a meaningful figure of merit (such as laser threshold density) has not been conducted. Turner *et al.* used uncracked Sb_4 and As_4, in order to control the As mole fraction the Sb_4 flux was varied with As_4 flux held constant [3-5]. They were able to demonstrate ~50 A/cm^2 threshold current density at λ~2 μm. This threshold density is comparable to the best observed quantum well laser results on any material system. Wagner and Weimann utilized cracked Sb_2 and As_2 with a constant Sb_2 flux sufficient to group-V stabilize the growth surface and controlled the As and Sb mole fractions by adjusting the As_2 flux [6-8]. They were able to realize 150 A/cm^2 threshold density with wall-plug efficiency of 23% at λ~2.26 μm and room temperature cw operation with > 240mW output power. Kaspi et al. report a method based on digital modulation of As flux where the duty cycle controls the As incorporation. They found the incorporation of As and thus the lattice mismatch was much less sensitive to the As flux in this case. Wen Wang's group at Columbia University implemented this technique, along with tensiley-strained barriers, to demonstrate λ ~ 2.38 μm lasers that operated in cw mode up to >100˚C, with room temperature threshold of 150 A/cm^2 [9]. This plethora of potential approaches for controlling the As and Sb mole fractions comes from the two incorporation mechanisms for As in GaSb-based alloys. Because of the excess group-V flux, there is direct competition for group-V sites. In addition, the III-Sb bond is relatively weak. This results in an As-for-Sb exchange reaction which enhances the As incorporation [10, 11]. The component from the exchange reaction is exponentially dependent on temperature, but also depends on As/Sb flux ratio and group-III growth rate. Because the alloy composition depends on growth temperature, group-III growth rate, group-V overpressure, and flux ratios, an exhaustive study of optical quality over the entire parameter space requires a prohibitive number of growths. We have restricted our investigation to low substrate temperatures for future integration with dilute nitride active region.

The basic laser structure that we will be implementing consists of claddings of $Al_{0.9}Ga_{0.1}As_{0.07}Sb_{0.93}$, separate confinement regions and barriers of $Al_{0.23}Ga_{0.42}In_{0.35}As_{0.32}Sb_{0.68}$ and multiple QWs of $Ga_{0.54}In_{0.46}As_ySb_{1-y}$. Calibrations for each alloy have been performed. Photoluminescence (PL) spectra for an AlGaAsSb/GaInAsSb quantum well structure grown at different substrate temperatures are shown in **Fig. 8**. We incorporated 3 monolayer layers of GaSb between cladding and core regions in order to allow us to change group-III temperatures to yield the desired alloy composition. This is not necessary between the barrier and quantum wells, as the Ga and In alloy compositions have been chosen to only require variation of the group-V flux between the two layers. This is accomplished by changing valve positions and requires only a few seconds.

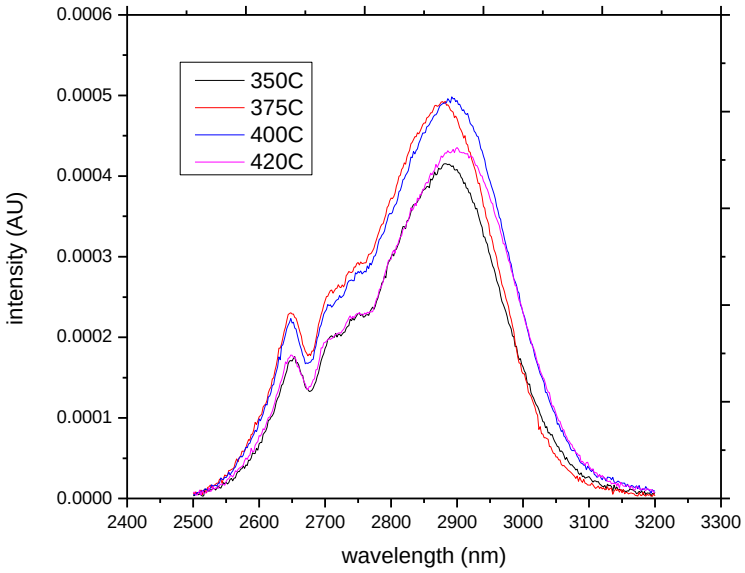

Figure 8. Room temperature photoluminescence spectra of single quantum well with varying growth temperature. Please note that the high-energy shoulder is caused by atmospheric effects.

Development of the laser structure is completed. Lattice-matching of the quinary barrier material was accomplished in a manner similar to that of Wagner and Weimann by growing with a constant Sb flux that is above stoichiometry and adjusting the As incorporation with the As/Sb flux ratio. In order to demonstrate the improved waveguide loss with integration of the nanoparticle-enhanced tunnel junctions, lattice-matched claddings have been developed in a similar manner.

By demonstrating reduced absorption loss at even relatively short wavelengths (~2.8 μm), we will be able to observe the potential of these tunnel junction claddings directly by measuring internal loss and threshold density of a laser. The benefit of removing a significant number of holes from the cladding will only increase with the emission wavelength of the laser active region (e.g. as we add nitrogen), as intervalance band absorption increases with the square of the emission wavelength.

5. References

[1] L. Shterengas, G. Belenky, M. V. Kisin, and D. Donetsky, "High power 2.4 μm heavily strained type-I quantum well GaSb-based diode lasers with more than 1 W of continuous wave output power and a maximum power-conversion efficiency of 17.5%," *Applied Physics Letters*, vol. 90, Jan 2007.

[2] J. S. M. Rattunde, C. Mermelstein, R. Keifer, and J. Wagner, "III-Sb-Based Type-I QW Diode Lasers," in *Mid-infrared Semiconductor Optoelectronics*, A. Krier, Ed., ed: Springer, 2006.

[3] H. K. Choi and S. J. Eglash, "High-efficiency high-power GaInAsSb-AlGaAsSb double-heterostructure lasers emitting at 2.3 μm," *Quantum Electronics, IEEE Journal of*, vol. 27, pp. 1555-59, 1991.

[4] H. K. Choi and S. J. Eglash, "High-power multiple-quantum-well GaInAsSb/AlGaAsSb diode lasers emitting at 2.1 mu m with low threshold current density," *Applied Physics Letters*, vol. 61, pp. 1154-56, 1992.

[5] S. J. Eglash, H. K. Choi, and G. W. Turner, "MBE growth of GaInAsSb/AlGaAsSb double heterostructures for infrared diode lasers," *Journal of Crystal Growth*, vol. 111, pp. 669-76, 1991.

[6] C. Mermelstein, S. Simanowski, M. Mayer, R. Kiefer, J. Schmitz, M. Walther, and J. Wagner, "Room-temperature low-threshold low-loss continuous-wave operation of 2.26 mu m GaInAsSb/AlGaAsSb quantum-well laser diodes," *Applied Physics Letters*, vol. 77, pp. 1581-83, 2000.
[7] S. Simanowski, C. Mermelstein, M. Walther, N. Herres, R. Kiefer, M. Rattunde, J. Schmitz, J. Wagner, and G. Weimann, "Growth and layer structure optimization of 2.26 [mu]m (AlGaIn)(AsSb) diode lasers for room temperature operation," *Journal of Crystal Growth*, vol. 227-228, pp. 595-99, 2001.
[8] S. Simanowski, M. Walther, J. Schmitz, R. Kiefer, N. Herres, F. Fuchs, M. Maier, C. Mermelstein, J. Wagner, and G. Weimann, "Arsenic incorporation in molecular beam epitaxy (MBE) grown (AlGaIn)(AsSb) layers for 2.0-2.5 [mu]m laser structures on GaSb substrates," *Journal of Crystal Growth*, vol. 201-202, pp. 849-53, 1999.
[9] W. Li, H. Shao, D. Moscicka, A. Torfi, and W. I. Wang, "Midinfrared InGaAsSb quantum well lasers with digitally grown tensile-strained AlGaAsSb barriers," 2007, pp. 1083-86.
[10] T. Brown, A. Brown, and G. May, "Anion exchange at the interfaces of mixed anion III--V heterostructures grown by molecular beam epitaxy," Sante Fe, New Mexico, 2002, pp. 1771-76.
[11] B. Z. Nosho, B. R. Bennett, L. J. Whitman, and M. Goldenberg, "Effects of As[sub 2] versus As[sub 4] on InAs/GaSb heterostructures: As-for-Sb exchange and film stability," in *28th conference on the physics and chemistry of semiconductor interfaces*, Lake Buena Vista, Florida (USA), 2001, pp. 1626-30.